European Journal of Radiology 121 (2019) 108718

Contents lists available at ScienceDirect

European Journal of Radiology

journal homepage: www.elsevier.com/locate/ejrad

Research article

Evaluating the HER-2 status of breast cancer using mammography radiomics features

Jing Zhou[a,b,d,1], Hongna Tan[a,b,1], Yan Bai[a,b], Jie Li[c], Qing Lu[a,b], Rushi Chen[a,b], Menghuan Zhang[a,b], Qin Feng[a,b], Meiyun Wang[a,b,*]

[a] Department of Radiology, Henan Provincial People's Hospital, Henan, 450003, China
[b] Imaging Diagnosis of Neurological Diseases and Research Laboratory of Henan Province, China
[c] Huiying Medical Technology Inc., Beijing, China
[d] Medical Imaging School, Mudanjiang Medical University, Mudanjiang, Heilongjiang Province, 157011, China

ARTICLE INFO

Keywords:
Breast cancer
HER-2
Radiomics
Mammography

ABSTRACT

Purpose: The aim of our study was to evaluate the HER-2 status in breast cancer patients using mammography (MG) radiomics features.

Methods: A total of 306 Chinese female patients with invasive ductal carcinoma of no special type (IDC-NST) enrolled from January 2013 to July 2018 were divided into a training set (n = 244) and a testing set (n = 62). One hundred and eighty-six radiomics features were extracted from digital MG images based on the training set. The least absolute shrinkage and selection operator (LASSO) method was used to select the optimal predictive features for HER-2 status from the training set. Both support vector machine (SVM) and logistic regression models were employed based on the selected features. The area under the receiver operating characteristic (ROC) curves (AUCs) of the training set and testing set were used to evaluate the predictive performance of the models.

Results: Compared with the SVM model, the performance of the logistic regression model using a combination of cranial caudal (CC) and mediolateral oblique (MLO) MG views was optimal. In the training set, the sensitivity, specificity, accuracy and area under the curve (AUC) values of the logistic regression model for evaluating HER-2 status based on quantitative radiomics features were 87.29%, 58.73%, 80.00% and 0.846 (95% confidence interval (CI), 0.800-0.887), respectively, and in the testing set, the values were 73.91%, 68.75%, 77.00% and 0.787 (95% CI, 0.673-0.885), respectively.

Conclusions: Radiomics features could be an efficient tool for the preoperative evaluation of HER-2 status in patients with breast cancer.

1. Introduction

Breast cancer is one of the most common cancers and is the main cause of cancer-related death among women worldwide [1]. The age-standardized incidence rate (ASR) for breast cancer is estimated to be 27 per 100 000 women-years in Asia [2], and breast cancer alone represents 30% of all new cancer diagnoses in women [3]. HER-2 amplification or overexpression was first identified in 1987 and is present in approximately 20–30 % of cases of human breast cancer [4]. The response to certain chemotherapies, such as taxanes and anthracyclines, can be predicted by HER-2 positivity [5,6]. Furthermore, patients with HER-2-positive breast cancer who are not treated with anti-HER-2 therapy will have a high risk of recurrence, specifically during the first 5 years after diagnosis [7]. Hence, the HER-2 amplification and overexpression status of breast cancer plays an important role in prognosis and treatment strategies. Currently, the two methods approved for determining HER-2 amplification and overexpression status in breast cancer patients are fluorescence in situ hybridization (FISH) and immunohistochemistry (IHC), which are performed on core-needle biopsy specimens [8]. However, due to the relatively small tissue specimen dimensions and tumor heterogeneity, evaluating HER-2 amplification and overexpression status in breast cancer based on a needle biopsy specimen may not be representative of the entire tumor. Some morphological and functional abnormalities have been identified by

* Corresponding author at: Department of Radiology, Henan Provincial People's Hospital, 450003; 7 Road, Weiwu Road, Jinshui District, Zhengzhou City, Henan Province, China.
E-mail address: marian9999@163.com (M. Wang).
[1] Jing Zhou and Hongna Tan contributed equally to this work.

https://doi.org/10.1016/j.ejrad.2019.108718
Received 20 January 2019; Received in revised form 6 September 2019; Accepted 18 October 2019
0720-048X/ © 2019 Published by Elsevier B.V.

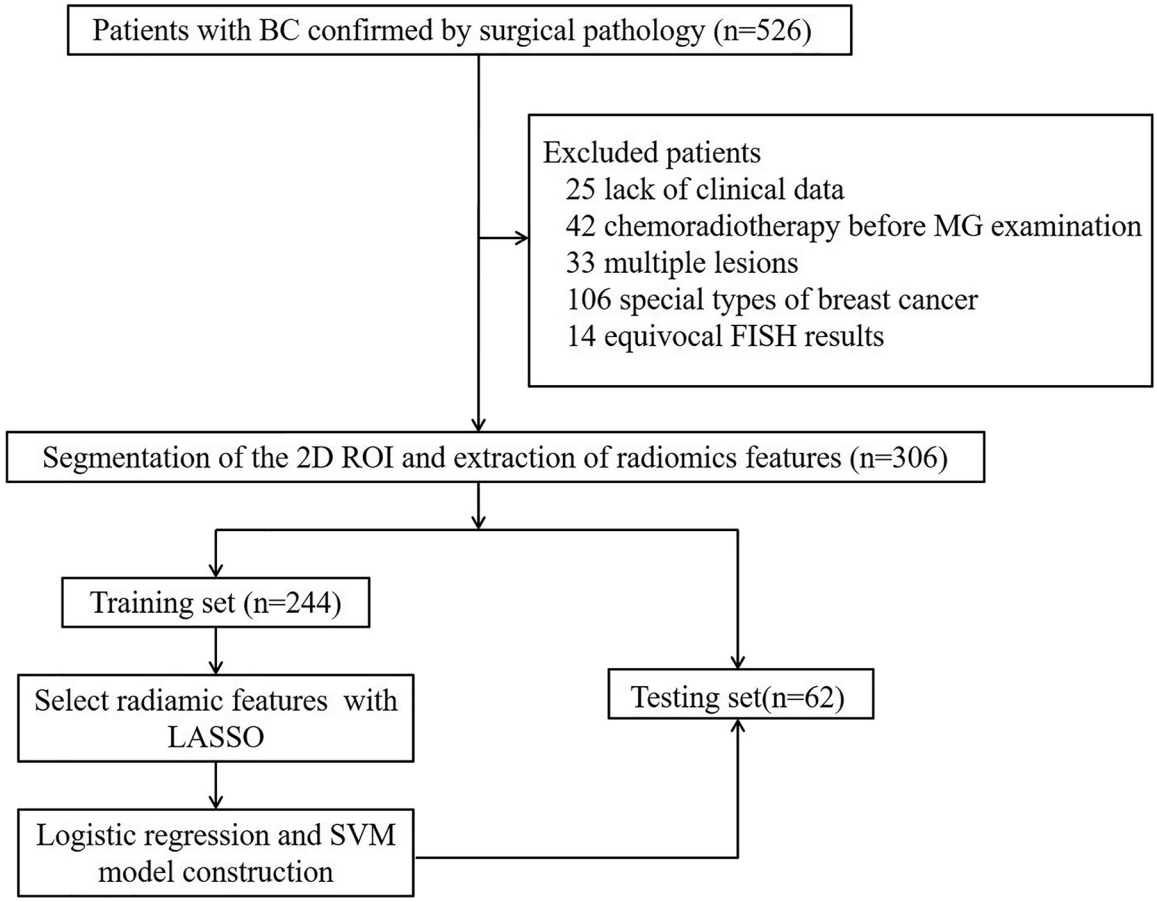

Fig. 1. Radiomics workflow and study flowchart.

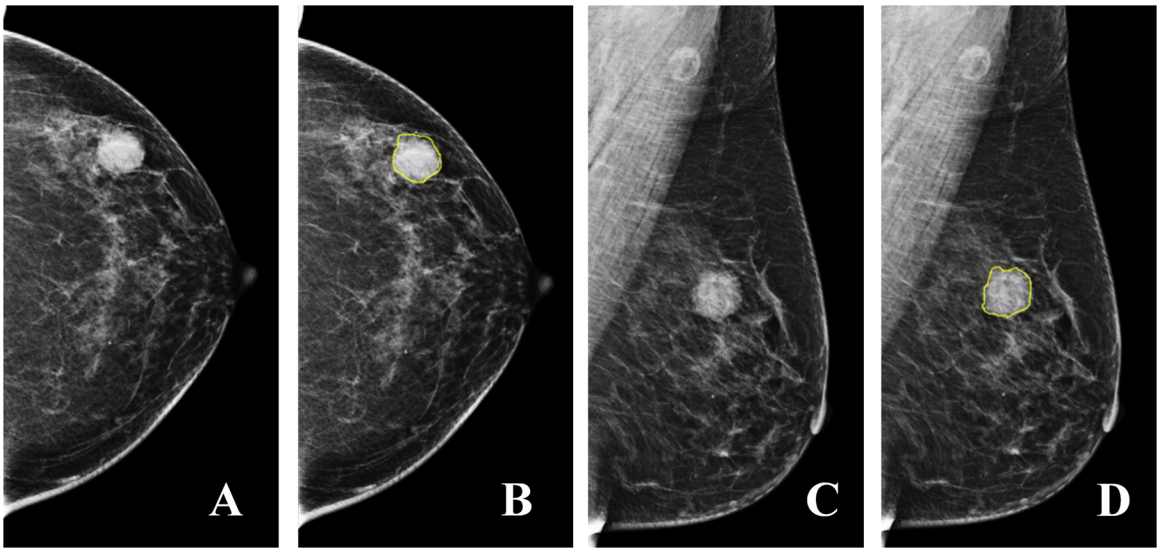

Fig. 2. A volume of interest (VOI) of breast cancer lesions was created manually on CC and MLO MG views. (A) A lobulated breast cancer mass is shown on the CC view mammogram. (B) The VOI of the breast cancer lesion was drawn manually on the same image. (C) A lobulated breast cancer mass is shown on the MLO view mammogram. (D) The VOI of the breast cancer lesion was drawn manually on the same image.

noninvasive imaging modalities and could be used in evaluating the HER-2 status of breast carcinoma [9], including mammography (MG), magnetic resonance imaging (MRI), and positron emission tomography/computed tomography (PET/CT). However, these imaging methods are cost-prohibitive for most breast cancer patients. More importantly, some of these modalities are unavailable in primary hospitals. Therefore, it is urgent for clinicians to identify a noninvasive and inexpensive imaging method to preoperatively evaluate the HER-2 status of breast cancer.

Radiomics is a rapidly emerging field of research that involves the extraction and analysis of quantitative features from abnormal lesions defined as signs of cancer on medical images [10], and it has enormous potential for improving the overall knowledge of tumor biology and for guiding the treatment of tumor patients. Some studies have found that

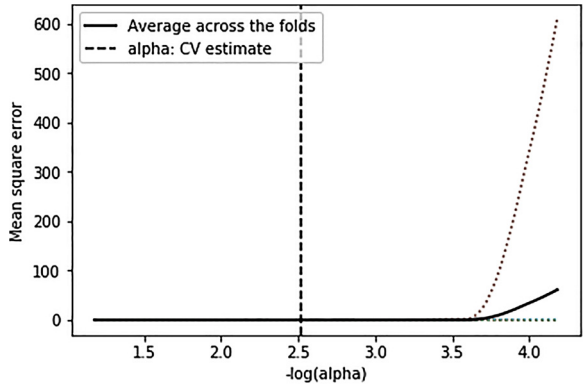

Fig. 3. Mean square error path diagram.
Notes: The optimization goal of LASSO is as follows:

$$\min_{\omega} \frac{1}{2n samples} ||Xw-y||_2^2+\alpha \ ||w||\ 1$$

The abscissa is -log(alpha), and the dotted lines in different colors indicate that each set of cross-verified samples has different mean square error for a different -log(alpha). The optimal alpha is the alpha value with the lowest mean square error of each group. The optimal alpha value was 0.003062, and -log(alpha) was 2.513944.

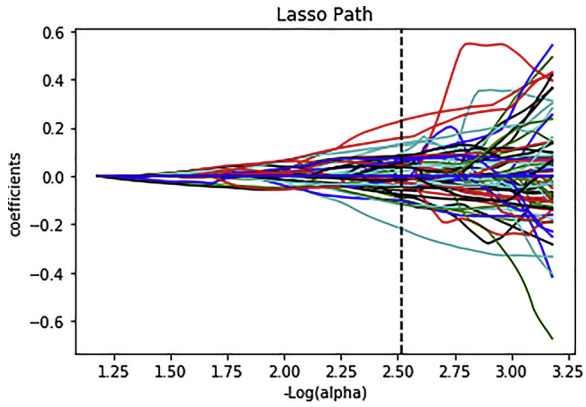

Fig. 4. LASSO coefficient solution path of the forty features.
The vertical axis represents the coefficients of each feature in the LASSO model. The coefficients vary with -log(alpha). According to the optimal -log(alpha), Forty features with nonzero coefficients were selected from 186 features.

molecular subtypes and gene-expression patterns are related to radiomics features, including intensity, shape and texture features, extracted from digital medical images through high-throughput computing in breast, lung and head-and-neck cancer [11,12]. The aim of our study is to predict preoperatively the HER-2 status of breast cancer using non-invasive radiomics methods, which will be helpful for clinician decision making.

2. Materials and methods

2.1. Study population

Ethical approval was obtained for this retrospective study, and the requirement for patient informed consent requirement was waived. Imaging data from a total of 526 patients who were initially diagnosed with invasive breast cancer were collected between January 2013 and June 2018 in the picture archiving and communication system (PACS) from our Department of Radiology. The inclusion criteria for the study were as follows: (1) invasive ductal carcinoma of no special type (IDC-NST) pathologically confirmed by surgery; (2) MG performed fewer than 20 days preoperatively with imaging quality that met the requirements for postprocessing; and (3) postoperative specimens used to evaluate the HER-2 status with IHC or FISH if showed a HER-2 result of 2+ according to IHC. The exclusion criteria were as follows: (1) lack of clinical data; (2) chemoradiotherapy before MG examination; (3) multiple lesions; (4) breast cancer other than IDC-NST; and (5) equivocal FISH results. A total of 306 consecutive patients met the inclusion and exclusion criteria and were divided into a training set and testing set at a ratio of 4:1 using computer-generated random numbers. A total of 244 patients were allocated to the training set (median age of 49 years), and 62 patients were allocated to the testing set (median age of 50 years). Clinical characteristics, such as age, tumor size, and pathological grade, were collected from the PACS.

2.2. HER-2 analysis of surgical pathological specimens

Two pathologists with 10 years of experience who specialized in breast pathology re-examined all of the breast carcinoma samples to confirm the HER-2 status. Under the current American Society of Clinical Oncology/College of American Pathologists (ASCO/CAP) guidelines, HER-2 IHC results of 0+ or 1+ were defined as HER-2 negative, and HER-2 IHC results of 3+ or 2+ with gene amplification by FISH were defined as HER-2 positive [8].

2.3. Image acquisition and tumor segmentation

The radiomics workflow is presented in Fig. 1. Standard 2D mammograms were acquired with Hologic Selenia (Hologic Medical Systems, Boston, USA). We used Digital Imaging and Communications in Medicine (DICOM) images of cranial caudal (CC) and mediolateral oblique (MLO) views that had been archived in the PACS without applying any preprocessing or normalization. All the MG imaging data were uploaded to the Radcloud platform (Huiying Medical Technology Co., Ltd, Beijing, China) to acquire the volume of interest (VOI) for further analysis. Outlines were drawn slightly within the border of the breast mass on CC and MLO views. The VOIs were drawn manually by two experienced radiologists with more than 10 years of experience in breast imaging. A sample of the manual VOI drawing is presented in Fig. 2. A total of 186 quantitative radiomics features, including 112 first-order, 15 shape features, 27 gray-level cooccurrence matrix (GLCM), 16 gray-level run length matrix (GLRLM), 16 gray-level size zone matrix (GLSZM) features were extracted from the MG imaging data.

2.4. Statistical analysis

The least absolute shrinkage and selection operator (LASSO) was used to select the optimal predictive features for HER-2 status from the training set. The cost function of the LASSO method is as follows:

$$\min_{w} \frac{1}{2n} ||Xw-y||_2^2+\alpha \ ||w||\ 1$$

Based on the training set, the optimal LASSO alpha parameter was set by 10-fold cross-validation. In addition, the features with nonzero coefficients were selected from the 186 quantitative radiomics features. Finally, 40 features were selected to construct a radiomics signature, including 11 first-order features, 10 shape features, 11 GLCM features and 8 GLSZM features (Figs. 3–5, Table 4).

Support vector machine (SVM) and logistic regression models were employed based on the selected features. The area under the receiver operating characteristic (ROC) curves (AUCs) of the training set and testing set were used to evaluate the predictive performance of the models. In addition, the sensitivity, specificity and accuracy were calculated.

Statistical analysis was performed with Statistical Package for the

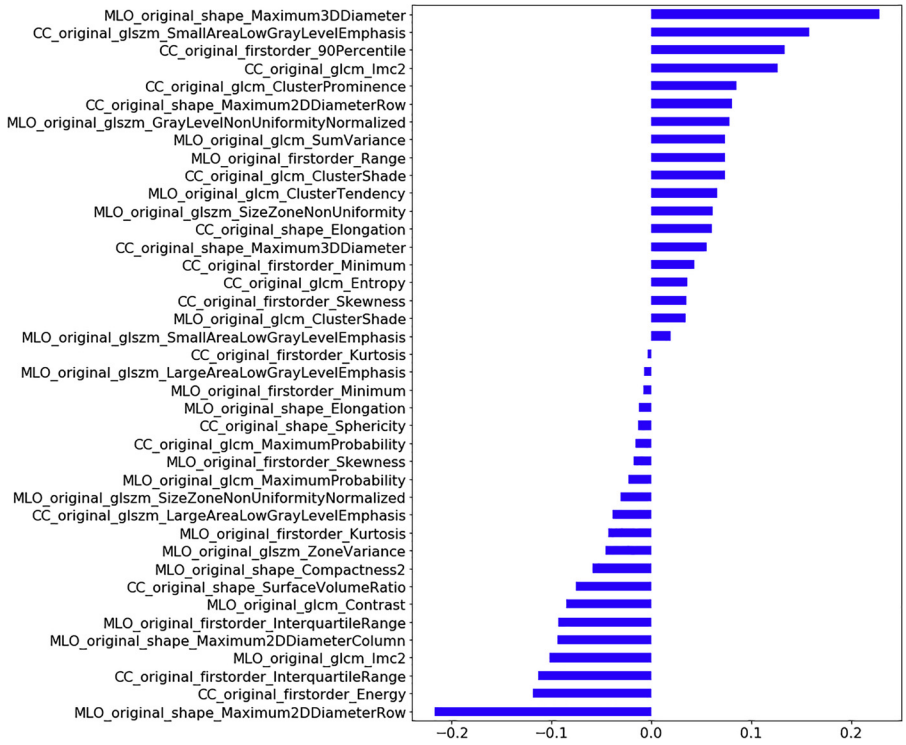

Fig. 5. Coefficients in the LASSO model of forty features.

Table 1
Clinicopathological features of patients with IDC-NST in the training and testing sets.

Clinicopathological features	Training set (n = 244)	Testing set (n = 62)	P value
Age (year, median)	49	50	0.452
Size (cm, $\bar{X} \pm s$)	2.486 ± 1.02	2.498 ± 1.01	0.932
BI-RADS density			0.784
Fatty	42(17.3%)	10(16.1%)	
Scattered	94(38.7%)	28(45.2%)	
Heterogeneous	80(32.9%)	19(30.6%)	
Extreme	27(11.1%)	5(8.1%)	
Pathological Grade			0.924
I	9(3.7%)	2(3.2%)	
II	143(58.6%)	35(56.5%)	
III	92(37.7%)	25(40.3%)	
Pathological ALN status			0.596
Positive	139(57%)	33(53.2%)	
Negative	105(43%)	29(46.8%)	
ER			0.306
Positive	170(69.7%)	39(62.9%)	
Negative	74(30.3%)	23(37.1%)	
PR			0.428
Positive	155(63.5%)	36(58.1%)	
Negative	89(36.5%)	26(41.9%)	
HER-2			0.998
Positive	63(25.8%)	16(25.8%)	
Negative	181(74.2%)	46(74.2%)	
Ki-67 index (%, $\bar{X} \pm s$)	43.54 ± 23.82	46.74 ± 22.38	0.341

Notes: BI-RADS, Breast Imaging Reporting and Data System; ER, estrogen receptor; PR, progesterone receptor; HER-2, human epidermal growth factor receptor-2; ALN, axillary lymph node.

Social Sciences (SPSS, version 22, Chicago, IL, USA). Statistical tests were all two-sided, and a P-value less than 0.05 was considered to indicate a statistically significant difference.

Table 2
Clinicopathological features of patients with HER-2-positive and HER-2-negative breast carcinoma.

Clinicopathological features	HER-2 status		P value
	Positive (n = 227)	Negative (n = 79)	
Age (year, median)	50	49	0.648
Size (cm, $\bar{X} \pm s$)	2.758 ± 1.12	2.395 ± 0.96	0.006
BI-RADS density			0.172
Fatty	9(11.4%)	43(18.9%)	
Scattered	32(40.5%)	91(40.1%)	
Heterogeneous	32(40.5%)	67(29.5%)	
Extreme	6(7.6%)	26(11.5%)	
Pathological Grade			0.279
I	2(2.5%)	9(4%)	
II	41(51.9%)	137(60.4%)	
III	36(45.6%)	81(35.7%)	
Pathological ALN status			0.270
Positive	36(45.6%)	136(59.9%)	
Negative	43(54.4%)	91(40.1%)	
ER			0.001
Positive	42(53.2%)	167(73.6%)	
Negative	37(46.8%)	60(26.4%)	
PR			0.000
Positive	34(43%)	157(69.2%)	
Negative	45(57%)	70(30.8%)	
Ki-67 index (%, $\bar{X} \pm s$)	42.67 ± 24.55	48.55 ± 19.82	0.056

Notes: BI-RADS, Breast Imaging Reporting and Data System; ER, estrogen receptor; PR, progesterone receptor; ALN, axillary lymph node.

3. Results

3.1. Patients characteristics

The basic demographic and clinical characteristics of the patients, including those included in the training and testing sets, are summarized in Table 1. There were no significant differences between the training and testing sets in terms of age, lesion size, gland density,

Table 3
Predictive performance of the models build from radiomics features from CC views alone, MLO views alone, and a combination of CC and MLO views.

Method	Training set (n = 244)				Testing set (n = 62)			
	Sensitivity	Specificity	Accuracy	AUC (95%CI)	Sensitivity	Specificity	Accuracy	AUC (95%CI)
logistic regression (CC)	68.50%	68.25%	75%	0.735 (0.679-0.790)	56.52%	62.5%	69%	0.656 (0.519-0.786)
logistic regression (MLO)	65.74%	65.07%	73%	0.732 (0.671-0.793)	54.34%	75%	73%	0.711 (0.592-0.818)
logistic regression (CC + MLO)	87.29%	58.73%	80%	0.846 (0.800-0.887)	73.91%	68.75%	77%	0.787 (0.673-0.885)
SVM (CC)	71.27%	65.07%	75%	0.709 (0.646-0.774)	50%	68.75%	69%	0.629 (0.486-0.773)
SVM (MLO)	69.06%	68.25%	75%	0.716 (0.649-0.785)	58.69%	68.75%	72%	0.655 (0.535-0.769)
SVM (CC + MLO)	83.97%	68.25%	81%	0.846 (0.796-0.891)	60.86%	68.75%	73%	0.740 (0.622-0.841)

Notes: CC, cranial caudal; MLO, mediolateral oblique.

Table 4
LASSO coefficient profiles of the forty features.

Features	Coefficients
MLO_original_shape_Maximum3DDiameter	0.228436
CC_original_glszm_SmallAreaLowGrayLevelEmphasis	0.158051
CC_original_firstorder_90Percentile	0.133864
CC_original_glcm_Imc2	0.126064
CC_original_glcm_ClusterProminence	0.085566
CC_original_shape_Maximum2DdiameterRow	0.081187
MLO_original_glszm_GrayLevelNonUniformityNormalized	0.077782
MLO_original_glcm_SumVariance	0.074014
MLO_original_firstorder_Range	0.073659
CC_original_glcm_ClusterShade	0.073454
MLO_original_glcm_ClusterTendency	0.065748
MLO_original_glszm_SizeZoneNonUniformity	0.061371
CC_original_shape_Elongation	0.061022
CC_original_shape_Maximum3Ddiameter	0.055588
CC_original_firstorder_Minimum	0.043408
CC_original_glcm_Entropy	0.035975
CC_original_firstorder_Skewness	0.035192
MLO_original_glcm_ClusterShade	0.034642
MLO_original_glszm_SmallAreaLowGrayLevelEmphasis	0.019054
CC_original_firstorder_Kurtosis	−0.00381
MLO_original_glszm_LargeAreaLowGrayLevelEmphasis	−0.00687
MLO_original_firstorder_Minimum	−0.00809
MLO_original_shape_Elongation	−0.01207
CC_original_shape_Sphericity	−0.01352
CC_original_glcm_MaximumProbability	−0.01543
MLO_original_firstorder_Skewness	−0.01716
MLO_original_glcm_MaximumProbability	−0.02269
MLO_original_glszm_SizeZoneNonUniformityNormalized	−0.03104
CC_original_glszm_LargeAreaLowGrayLevelEmphasis	−0.03872
MLO_original_firstorder_Kurtosis	−0.04323
MLO_original_glszm_ZoneVariance	−0.04554
MLO_original_shape_Compactness2	−0.05902
CC_original_shape_SurfaceVolumeRatio	−0.07558
MLO_original_glcm_Contrast	−0.08545
MLO_original_firstorder_InterquartileRange	−0.09291
MLO_original_shape_Maximum2DdiameterColumn	−0.09353
MLO_original_glcm_Imc2	−0.10217
CC_original_firstorder_InterquartileRange	−0.11324
CC_original_firstorder_Energy	−0.11829
MLO_original_shape_Maximum2DdiameterRow	−0.21701

pathological grade, estrogen receptor (ER) status, progesterone receptor (PR) status, HER-2 status, or Ki-67 proliferation index (all $P > 0.05$).

Of the 306 patients with IDC-NST who were included in our study, 227 (74.2%, 227/306) had HER-2-negative breast cancer, and 79 (25.8%, 79/306) had HER-2-positive breast cancer. The results of the clinicopathological features between the patients with negative and positive HER-2 status are listed in Table 2. The size of the breast cancer lesions and ER/PR status were significantly different between patients with HER-2-positive and HER-2-negative breast cancer ($P = 0.006$, $P = 0.001$ and $P = 0.000$, respectively). The features of age, gland density, pathological grade, pathological axillary lymph node (ALN) status, and Ki-67 proliferation index showed no differences between HER-2-positive and HER-2-negative breast cancer ($P = 0.648$, $P = 0.172$, $P = 0.279$, $P = 0.27$ and $P = 0.056$, respectively).

3.2. Predicting HER-2 status based on mammographic radiomics features

The diagnostic efficacies of two models built using radiomics features from CC views alone, MLO views alone, and the combination of CC and MLO views are summarized in Table 3. Comparing the SVM and logistic regression models built from radiomics features from CC views alone, MLO views alone and CC and MLO views in combination, the logistic regression model built from a combination of features from CC views and MLO views showed the optimal performance for distinguishing HER-2 status. The sensitivity, specificity, accuracy and AUC values were 87.29%, 58.73%, 80.00% and 0.846 in the training set, respectively, and were 73.91%, 68.75%, 77.00% and 0.787 in the testing set, respectively. The sensitivity, specificity, accuracy and AUC values for predicting HER-2 status using the SVM model build from radiomics features from the combination of CC views and MLO views were 83.93%, 68.25%, 81.00%, and 0.846 in the training set, respectively, and were 60.86%, 68.75%, 73.00% and 0.740 in the testing set, respectively. ROC curves of the logistic regression model using the CC, MLO views and their combination are presented in Fig. 6A–F.

4. Discussion

HER-2 positivity in patients with breast carcinoma, namely, overexpression and/or amplification of the HER-2 receptor, is associated with more aggressive tumor phenotypes, malignant transformation of cells, poor clinical outcomes [13] and increased resistance to endocrine therapy [14]. In the large NOAH study, there was a statistically significant difference in the 3-year event-free survival (EFS) in patients with HER-2-positive breast cancer who were treated with or without trastuzumab, which is one of the most common HER-2-targeted therapies (71% vs. 56%; $P = 0.013$) [15]. Because treatment with trastuzumab benefits breast carcinoma with HER-2 amplification and overexpression [16], testing for HER-2 status is crucial for guiding therapy.

In recent years, several studies have investigated the correlation between abnormal imaging features and HER-2 status [9,17–22]. Gajdos et al. reported that calcification on mammograms increased the likelihood of HER-2-positive status [18], especially in heterogeneous lesions and those with pleomorphic calcifications on MG ($P = 0.0078$ and $P = 0.0002$, respectively) [23]. Another previous study indicated

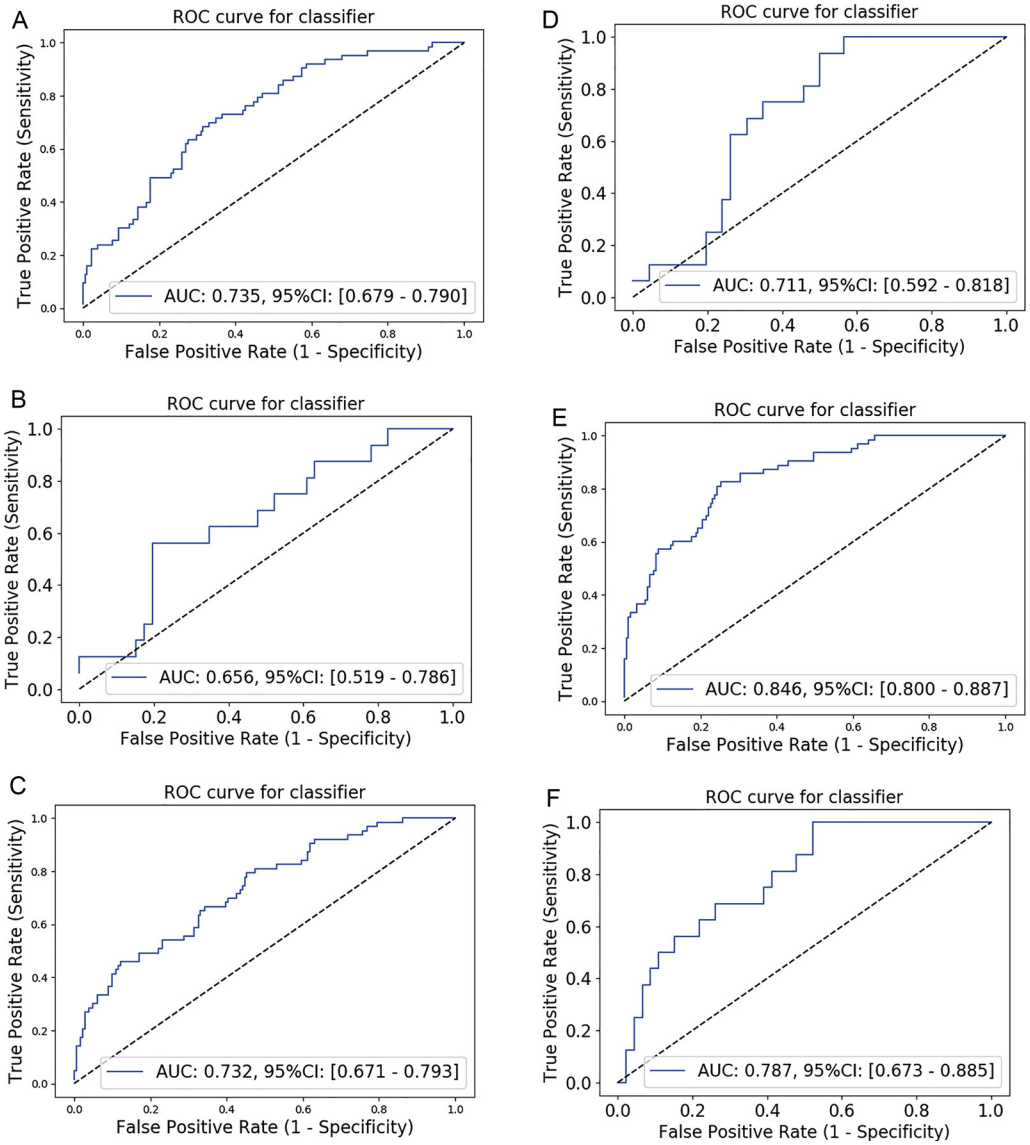

Fig. 6. ROC curves from the logistic regression model for predicting the HER-2 status of breast cancer patients.
Curves were constructed from radiomics features from CC views alone (A–B), MLO views alone (C–D) and a combination of CC and MLO views (E–F) in the training set and testing set, respectively.
Notes: AUC, area under the curve; ROC, receiver operating characteristic; CC, cranial caudal; MLO, mediolateral oblique.

that a mass with indistinct margins, calcifications within a mass and segmental calcifications on MG were significantly related to HER-2 positivity ($P = 0.011$, $P < 0.001$ and $P = 0.030$, respectively) [24]. A published meta-analysis revealed that the presence of microcalcifications, microcalcifications with a branching or fine linear morphology, BI-RADS breast density category 4 (extremely dense) and a high mammographic suspicion of malignancy were significantly associated with HER-2 overexpression ($P < 0.001$, $P = 0.03$, $P = 0.01$ and $P < 0.01$, respectively) [9]. Although a certain correlation existed between MG imaging features and HER-2 status, the results are somewhat heterogenous, which might be a result of confounders in some studies, such as tumor size, pathological grade, pathological ALN status, and hormone receptor status. Hence, the value of MG for preoperative prediction of HER-2 status is very limited and lacks accuracy.

In this study, we developed and validated two radiomics models, namely, an SVM and a logistic regression model, using MG to predict HER-2 status in patients with breast carcinoma to support clinical decision-making. The performance of both models based on radiomics features from CC views alone, MLO views alone and a combination of CC and MLO views were compared, and the optimal predictive performance was obtained with the logistic regression model built using radiomics features from a combination of CC and MLO MG views, with an AUC of 0.846 in the training set and an AUC of 0.787 in the testing set. A study by Li et al. showed that computer-extracted tumor phenotypes using quantitative radiomics features from MRI had poor the efficacy for determining HER-2 status, with an AUC value of 0.65, which was far less than that of our model [25]. This finding may be because IHC alone was used to identify HER-2 status in this study, and the study was based on a small samples (n = 91). A previous study using quantitative radiomics features from digital MG to predict molecular subtype, and three binary classifications of the subtypes were used to predict luminal (A + B) vs nonluminal, HER-2-enriched vs non-HER-2-enriched, and triple-negative vs non-triple-negative breast cancer. The AUC/accuracy of the three binary classifications were 0.752/0.788, 0.784/0.748 and 0.865/0.796 [11]. Our prediction model for HER-2 status performed better than the binary classifier from the previous study for HER-2-enriched vs non-HER-2-enriched breast cancer [11]. The reason may be related to the different criteria for

molecular subtypes used in our study and their study because non-HER-2-enriched breast cancer includes the luminal-B subtype, in which HER-2 may be amplified or overexpressed according to the criteria of the 2013 St. Gallen International Breast Cancer Conference [26]. Our study suggests that a classifier developed from quantitative radiomics features extracted from MG shows promise as a noninvasive method for high-throughput image-based phenotyping to determine HER-2 status in breast cancer.

However, our study has several limitations. First, we included only IDC-NST in this study because this pathological type is the most common. Second, correlations among other prognostic factors of breast cancer and radiomics features were not analyzed because these other prognostic factors, such as ER status, PR status and Ki-67 index, are less correlated with targeted therapeutic decisions. Third, multimodal radiomics models were not used in our study because of the lack of imaging data for the same patient. Finally, our results were based on data from a single center; thus, the reproducibility and generalization of the model must be validated further using other datasets.

In conclusion, the results of our study indicated that quantitative imaging features extracted from digital MG can potentially be used as a noninvasive and convenient tool to evaluate the HER-2 status of breast cancer patients. Further studies involving larger patient populations, multiple centers and multimodal imaging methods are still needed to confirm the correlation between quantitative imaging features and HER-2 status.

Funding

This work was supported by the National Natural Science Foundation of China (Nos. 81601466; 81720108021; 81271565; 81401378), Henan Provincial Department of Science and Technology Research Project (No. 201602221) and The Research and Innovation Foundation for Postgraduates of Mudanjiang Medical University (2017YJSCX-31MY).

Declaration of Competing Interest

The authors have no conflicts of interest to declare.

References

[1] I.O. Wong, C.M. Schooling, B.J. Cowling, et al., Breast cancer incidence and mortality in a transitioning Chinese population: current and future trends, Br. J. Cancer 112 (1) (2015) 167–170.
[2] J. Ferlay, I. Soerjomataram, R. Dikshit, et al., Cancer incidence and mortality worldwide: sources, methods and major patterns in GLOBOCAN 2012, Int. J. Cancer 136 (5) (2015) E359–386.
[3] R.L. Siegel, K.D. Miller, A. Jemal, Cancer statistics, 2018, CA Cancer J. Clin. 68 (1) (2018) 7–30.
[4] H.J. Burstein, The distinctive nature of HER2-positive breast cancers, N. Engl. J. Med. 353 (16) (2005) 1652–1654.
[5] L.G. Dressler, D.A. Berry, G. Broadwater, et al., Comparison of HER2 status by fluorescence in situ hybridization and immunohistochemistry to predict benefit from dose escalation of adjuvant doxorubicin-based therapy in node-positive breast cancer patients, J. Clin. Oncol. 23 (19) (2005) 4287–4297.
[6] D.F. Hayes, A.D. Thor, L.G. Dressler, et al., HER2 and response to paclitaxel in node-positive breast cancer, N. Engl. J. Med. 357 (15) (2007) 1496–1506.
[7] K. Strasser-Weippl, N. Horick, I.E. Smith, et al., Long-term hazard of recurrence in HER2+ breast cancer patients untreated with anti-HER2 therapy, Breast Cancer Res. 17 (2015) 56.
[8] A.C. Wolff, M.E. Hammond, D.G. Hicks, et al., Recommendations for human epidermal growth factor receptor 2 testing in breast cancer: American Society of Clinical Oncology/College of American Pathologists clinical practice guideline update, J. Clin. Oncol. 31 (31) (2013) 3997–4013.
[9] S.G. Elias, A. Adams, D.J. Wisner, et al., Imaging features of HER2 overexpression in breast cancer: a systematic review and meta-analysis, Cancer Epidemiol. Biomark. Prev. 23 (8) (2014) 1464–1483.
[10] F. Valdora, N. Houssami, F. Rossi, et al., Rapid review: radiomics and breast cancer, Breast Cancer Res. Treat. 169 (2) (2018) 217–229.
[11] W. Ma, Y. Zhao, Y. Ji, et al., Breast cancer molecular subtype prediction by mammographic radiomic features, Acad. Radiol. (2018), https://doi.org/10.1016/j.acra.2018.01.023.
[12] H.J. Aerts, E.R. Velazquez, R.T. Leijenaar, et al., Decoding tumour phenotype by noninvasive imaging using a quantitative radiomics approach, Nat. Commun. 5 (2014) 4006.
[13] W. Tai, R. Mahato, K. Cheng, The role of HER2 in cancer therapy and targeted drug delivery, J. Control. Release 146 (3) (2010) 264–275.
[14] R.H. Engel, V.G. Kaklamani, HER2-positive breast cancer: current and future treatment strategies, Drugs 67 (9) (2007) 1329–1341.
[15] L. Gianni, W. Eiermann, V. Semiglazov, et al., Neoadjuvant chemotherapy with trastuzumab followed by adjuvant trastuzumab versus neoadjuvant chemotherapy alone, in patients with HER2-positive locally advanced breast cancer (the NOAH trial): a randomised controlled superiority trial with a parallel HER2-negative cohort, Lancet 375 (9712) (2010) 377–384.
[16] K.A. Goddard, S. Weinmann, K. Richert-Boe, et al., HER2 evaluation and its impact on breast cancer treatment decisions, Public Health Genomics 15 (1) (2012) 1–10.
[17] P.A. Baltzer, T. Vag, M. Dietzel, et al., Computer-aided interpretation of dynamic magnetic resonance imaging reflects histopathology of invasive breast cancer, Eur. Radiol. 20 (7) (2010) 1563–1571.
[18] C. Gajdos, P.I. Tartter, I.J. Bleiweiss, et al., Mammographic appearance of non-palpable breast cancer reflects pathologic characteristics, Ann. Surg. 235 (2) (2002) 246–251.
[19] D. Groheux, S. Giacchetti, J.L. Moretti, et al., Correlation of high 18F-FDG uptake to clinical, pathological and biological prognostic factors in breast cancer, Eur. J. Nucl. Med. Mol. Imaging 38 (3) (2011) 426–435.
[20] S.H. Kim, B.K. Seo, J. Lee, et al., Correlation of ultrasound findings with histology, tumor grade, and biological markers in breast cancer, Acta Oncol. 47 (8) (2008) 1531–1538.
[21] Z. Nie, J. Wang, X.C. Ji, Microcalcification-associated breast cancer: HER2-enriched molecular subtype is associated with mammographic features, Br. J. Radiol. (2018) 20170942, , https://doi.org/10.1259/bjr.20170942.
[22] S. Ueda, H. Tsuda, H. Asakawa, et al., Clinicopathological and prognostic relevance of uptake level using 18F-fluorodeoxyglucose positron emission tomography/computed tomography fusion imaging (18F-FDG PET/CT) in primary breast cancer, Jpn. J. Clin. Oncol. 38 (4) (2008) 250–258.
[23] T.A. Patel, M. Puppala, R.O. Ogunti, et al., Correlating mammographic and pathologic findings in clinical decision support using natural language processing and data mining methods, Cancer 123 (1) (2017) 114–121.
[24] H.J. Shin, H.H. Kim, M.O. Huh, et al., Correlation between mammographic and sonographic findings and prognostic factors in patients with node-negative invasive breast cancer, Br. J. Radiol. 84 (997) (2011) 19–30.
[25] H. Li, Y. Zhu, E.S. Burnside, et al., Quantitative MRI radiomics in the prediction of molecular classifications of breast cancer subtypes in the TCGA/TCIA data set, NPJ Breast Cancer (2016) 2.
[26] A. Goldhirsch, E.P. Winer, A.S. Coates, et al., Personalizing the treatment of women with early breast cancer: highlights of the St Gallen International Expert Consensus on the Primary Therapy of Early Breast Cancer 2013, Ann. Oncol. 24 (9) (2013) 2206–2223.